

Manuscript version: Author's Accepted Manuscript

The version presented in WRAP is the author's accepted manuscript and may differ from the published version or Version of Record.

Persistent WRAP URL:

<http://wrap.warwick.ac.uk/152820>

How to cite:

Please refer to published version for the most recent bibliographic citation information.

Copyright and reuse:

The Warwick Research Archive Portal (WRAP) makes this work by researchers of the University of Warwick available open access under the following conditions.

Copyright © and all moral rights to the version of the paper presented here belong to the individual author(s) and/or other copyright owners. To the extent reasonable and practicable the material made available in WRAP has been checked for eligibility before being made available.

Copies of full items can be used for personal research or study, educational, or not-for-profit purposes without prior permission or charge. Provided that the authors, title and full bibliographic details are credited, a hyperlink and/or URL is given for the original metadata page and the content is not changed in any way.

Publisher's statement:

Please refer to the repository item page, publisher's statement section, for further information.

For more information, please contact the WRAP Team at: wrap@warwick.ac.uk.

Insights into the Emerging Networks of Voids in Simulated Supercooled Water

Narjes Ansari,^{*,†} Berk Onat,[‡] Gabriele C. Sosso,[‡] and Ali Hassanali^{*,†}

[†]*The Abdus Salam International Centre for Theoretical Physics, Strada Costiera 11, 34151 Trieste, Italy*

[‡]*Department of Chemistry and Centre for Scientific Computing, University of Warwick, Gibbet Hill Road, Coventry, CV4 7AL, United Kingdom*

[¶]*School of Engineering, University of Warwick, Gibbet Hill, Coventry CV4 7AL, United Kingdom*

E-mail: ansari.narjes@gmail.com; ahassana@ictp.it

Abstract

The structural evolution of supercooled liquid water as we approach the glass transition temperature continues to be an active area of research. Here, we use molecular dynamics simulations of TIP4P/Ice to study the changes in the connected regions of empty space within the liquid which we interrogate using the Voronoi-voids network. We observe two important features: supercooling enhances the fraction of non-spherical voids and different sizes of voids tend to cluster forming a percolating network. By examining order parameters such as the local structure index (LSI), tetrahedrality and topological defects, we show that water molecules near large void clusters tend to be slightly more tetrahedral than those near small voids, with a lower population of under- and over-coordinated defects. We show further that the distribution of closed rings of water molecules around small and large void clusters maintain a balance between 6

and 7 membered rings. Our results highlight the changes of the dual voids and water network as a structural hallmark of supercooling which provides insights into the molecular origins of cooperative effects that underlie density fluctuations occurring on the sub-nanometer and nanometer length scale. The percolation of the voids and the hydrogen bond network around the voids, may serve as useful order parameters to investigate density fluctuations in supercooled water.

Introduction

The physical properties of supercooled liquids are keys to understand the emergence of amorphous solids as well as the occurrence of crystal nucleation.^{1,2} The case of supercooled water is of special importance, as it underpins countless practical applications ranging from the vitrification of glassy water in the context of cryopreservation,³ to the formation of ice in our atmosphere.⁴

Understanding the molecular origins of anomalies in water particularly upon supercooling has been a subject of numerous experimental and theoretical studies.^{5–14} One of the important hallmarks of interpreting many of the anomalies in water and its rich phase diagram has been to analyse the polymorphic character that water appears to acquire at low temperature and pressures. In particular, the hypothesized existence of a liquid-liquid critical point (LLCP) is rationalized by the presence of two liquids: high density liquid (HDL) and low density liquid (LDL) that are in quasi-equilibrium with each other which has been suggested by various experiments.^{15–20} Numerous simulations also support the existence of the LLCP.^{21–30} Occurrence of these two liquids is further backed-up by the presence of two amorphous states of ice namely low and high density amorphous ice (LDA and HDA) which can be interpreted as the glassy analogs of LDL and HDL.^{31–33} There have also been various spectroscopic experiments verify the existence and strengthen the evidences of two states in liquid water.^{34–38}

Theory and simulations have played important roles in portraying the molecular picture

of HDL and LDL water. A popular approach to study this has been the structure analysis with inherent potential energy surface (IPES) where configurations are sampled by quenching to 0 K with finite temperature molecular dynamics and water molecules with different hydrogen bond environments are identified using these samples.³⁹ Several different types of metrics or order parameters have been used to characterize the local hydrogen bond patterns around LDL and HDL-like water.⁵ Some of the popular ones include the local structure index (LSI) employed in Ref. 40 and the tetrahedrality (q).^{41,42} These and other parameters give structural signatures in the hydrogen bond network that occurs on a short length scale involving mostly the first solvation shell. In a recent work, Martelli⁴³ has nicely illustrated the importance of global order parameters in the evolution of supercooled water. Specifically, the study shows that the LDL and HDL-like water molecules as defined by the LSI, are characterized by a collective effect involving clustering of LDL and HDL-like environments.⁴³

In a similar spirit with this work,⁴³ we have recently characterized the properties of empty space in liquid water. Using the Voronoi-void network we have found that liquid water is characterized by a large proportion of small spherical voids and large fractal or dendritic like voids at ambient conditions.⁴⁴ Voids have allowed us to identify the inhomogeneities in density, generated by fluctuations in a manner where anisotropies can be *seen* in a very chemically intuitive manner. The use of Voronoi-voids to examine the role of geometry on packing in simple liquids has previously been highlighted by Sastry and co-workers.⁴⁵

In this report we build on our earlier works,^{44,46–48} we investigating the evolution of the Voronoi-void network of water upon supercooling. In our earlier work using simulations with TIP4P/Ew, we showed that equilibrium fluctuations create transient inhomogeneities by the spherical and non-spherical shaped voids. Herein, using classical molecular dynamics simulations, we study how water-void dual network changes upon supercooling TIP4P/Ice⁴⁹ in the temperature range between 230-260 K. Two interesting features emerge from our analysis: first, supercooling results in a subtle increase in the fraction of large non-spherical dendritic voids and second voids appear to cluster as water goes into the supercooled regime

implying the creation of large connected regions of empty space that cover up to ~ 8 nm length scales. Using the voids-network, we find that water molecules near isolated voids are slightly less tetrahedral than those near large connected voids. We also show that, the population of water molecules associated with under- (2A-1D, 1A-2D) and over-coordinated (3A-2D, 2A-3D) topological defects is lower near the large connected voids. By examining hydrogen bonded rings near the voids, we determine that there is an enhancement of hexagonal rings around the large connected voids consistent with previous studies.^{39,43,50}

The paper is organised as follows: in the first section we illustrate the basics of the computational methods we have used to investigate voids (Sec. "Voronoi Voids") and networks of voids (Sec. "Voids networks") in supercooled liquid water. In sections "Voids in Supercooled Liquid Water", "The Percolating Voids Network" and "The Water Network Near Voids", we illustrate the features of the voids as a function of supercooling, discuss the emergence of networks of voids, and proceed to investigate the structural properties of water molecules at the interface with different classes of voids networks, respectively. In Section "HD/LD Liquid Water and the Void Network", we discuss how interplay between LD and HD water, which has been proposed to be correlated with the Stokes-Einstein relation (SER) breakdown in supercooled liquid water, can possibly be rationalised in terms of the voids network. Finally, we provide our conclusions and perspectives.

Computational Methods

Molecular Dynamics Simulations

Molecular dynamics simulations have been performed using the GROMACS 5.1.4 package.⁵¹ Our models of supercooled liquid water contain 4500 TIP4P/Ice⁴⁹ molecules. This is an all-atom, rigid, non-polarizable water model that is widely accepted as one of the best possible options when dealing with simulations of supercooled liquid water and ice.^{50,52,53} We note that in Ref. 44 we have thoroughly validated the robustness of our results by using a diverse

portfolio of water models, including the very accurate framework of Paesani et al.;⁵⁴⁻⁵⁶ as such, we have no reason to believe that the usage of a specific water model would impact the soundness of our findings in this work. The geometry of the TIP4P/Ice model is enforced by means of the SETTLE algorithm⁵⁷ with H-bonds constraint is applied with P-LINCS algorithm.^{58,59} The cutoff for the non-bonded interactions is 1.2 nm and the long-range electrostatic interactions are computed using the particle-mesh Ewald algorithm⁶⁰ with the same cutoff. The equations of motion have been integrated using the velocity-Verlet algorithm⁶¹ with a time step of 2 fs. We use two different thermostats namely Nose-Hoover^{62,63} and Berendsen⁶⁴ in our simulations. The coupling constants of the two thermostats and the Parrinello-Rahman⁶⁵ barostat are 2, 2 and 4 ps, respectively.

We have generated several different models of supercooled liquid water at 260, 250, 240 and 230 K, starting from an equilibrated trajectory obtained at room temperature for a cubic simulation box of $51.4 \times 51.4 \times 51.4 \text{ \AA}^3$. We have decided to sample the NPT ensemble to ensure an accurate representation of the density fluctuations within the system. In order to investigate possible effects of the cooling protocol when equilibrating our models at strong supercooling, we have adopted two different protocols: a linear cooling ramp and a step-wise cooling ramp. The former involves gradually lowering the temperature from e.g. 260 K to 250 K in 10 ns, while the latter requires a series of shorted (2 ns) equilibrations at the end of which the temperature is abruptly lowered by 2 K. The effect of different thermostats has also been probed - no significant effects or artifacts have emerged. A further 10 ns NPT simulation is incorporated at target temperatures for each cooling step and our analyses are carried out on additional 50 ns NPT simulations.

Voronoi Voids

To characterize the regions of empty space within the water network, we have computed the so-called Voronoi-Delaunay (VD) voids⁶⁶ using a framework, based on the VNP code.⁶⁷ We have previously developed and validated this framework in the context of density fluctuations

of liquid water at room temperature.⁴⁷ The key feature of said framework is that it allows us to identify voids of arbitrary shape and size - as opposed to spherical cavities only. Two parameters are important when defining the network of voids in a given system: bottleneck radius (R_B) and probe radius (R_P). While R_P controls the minimum size of the voids, R_B determines the extent of the area needed for two voids to be merged together as a single void. For consistency, we have used $R_B = 1.1$ and $R_P = 1.2$ Å as we have used in our previous work in Ref. 47. It is important to note that we have examined different R_B and R_P values and found no significant effect on our results, which is extensively discussed in our previous works.^{44,47} We urge interested readers to Ref. 68 and our reference works^{44,47} for more details on our framework and for a complete analyses of the effects of different parameters on the morphology of voids in liquid water.

We also examined the ring distributions of water molecules within 2 Å of the voids. In particular, we investigated primitive rings using the R.I.N.G.S. code.⁶⁸ Here a H-bond criteria of O-O distance < 3.5 Å and H-O...O angles $< 30^\circ$ is used to connect water molecules.

Voids networks

In order to investigate the connectivity of the voids network, the voids are mapped onto the nodes of a graph whose edges correspond to connections between different voids. Similar ideas have been used previously in the context of the analysis of the hydrogen bond network in molecular systems.⁶⁹ The voids identified via our methodology consist of combinations of polyhedra: if two voids share at least one vertex, a value of one is assigned to the corresponding edge of the graph - if not, the two voids are not considered as connected, and a value of zero is assigned to the corresponding edge. In the former case, the geometric distance between the closest pair of vertexes belonging to the voids (polyhedra) is zero, while in the latter, it is greater than zero (see panel a of Fig. 2).

As a result of this procedure, we obtain a graph which is representative of the entire network of the voids in the system. A depth-first search algorithm⁷⁰ (available in Matlab⁷¹)

is then used to post-process said graph to identify connected sub-graphs - i.e. *clusters* of connected voids. The tree-like graph depicted in Fig. 2c provides an example of a connected sub-graph of voids within a configuration of supercooled liquid water at 230 K.

Results

Voids in Supercooled Liquid Water

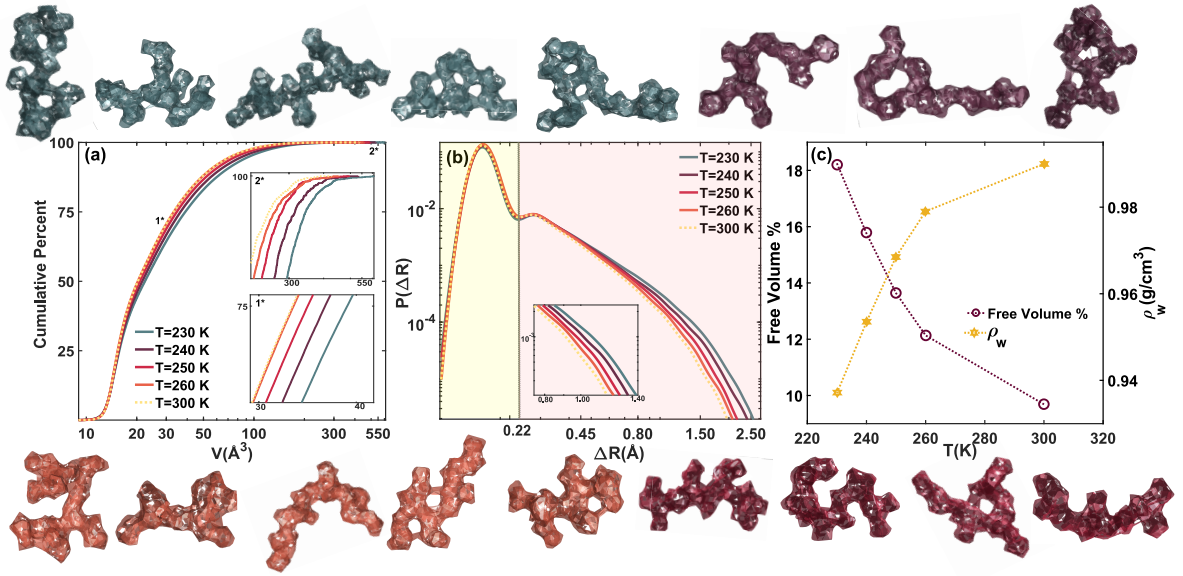


Figure 1: a) Cumulative distribution of the volumes of the voids at different temperatures (the x-axis is in log scale). The insets show a portion of the same graph for volumes between 30-40 \AA^3 (bottom inset) and 250-550 \AA^3 (top inset). The lower the temperature, the larger the voids are likely to be, b) the log-log plot of distribution of ΔR , i.e. a parameter that characterizes the morphology of a void to the spherical or non-spherical shape - see text. Regions of the graph corresponding to spherical and non-spherical voids are shaded in yellow and red, respectively. A representative example of a spherical and a non-spherical void is illustrated in panel c), and represents the free volume (left y-axis) and bulk density (right y-axis) of our models of supercooled water as a function of temperature. Surrounding the figure, we show examples of the large non-spherical voids in supercooled water at different temperatures. The color of each void corresponds to the color of legends in panel a) for each temperature.

In recent works^{44,48} we have shown that VD voids provide a very powerful framework for investigating the role of non-spherical cavities associated with density fluctuations in liquid

water. In particular, the voids and their water environment allow for the identification of high and low density regions generated by fluctuations on the sub-picosecond timescale. In the following, we elucidate how these structural features of the liquid change as we cool down water from room temperature to both mild and strong supercooling regimes.

As expected, taking water from 260 to 230 K lowers the density from 0.979 to 0.937 g/cm³ due to an increase in the free volume. In the following, we establish using the VD voids the microscopic origin associated with this change in the free volume. The left panel of Fig. 1 shows the cumulative distributions of the volumes of the voids obtained at 5 different temperatures: 300, 260, 250, 240 and 230 K. The distribution of the volumes clearly shows that the vast majority of the voids in both supercooled and ambient temperatures have small volume (Here, nearly 60 % of voids have a volume of less than 25 Å³). Although the effects appears to be rather subtle, the insets show that the probability of finding large voids steadily increases as a function of supercooling.

In our earlier study^{44,48} we have demonstrated that not just the size, but the morphology as well of the voids can have a huge impact on the structural properties of the liquid network: in particular, whether or not a given void can be considered close-to-spherical shape is quite key to the energetics associated with the corresponding density fluctuation. Thus, in order to assess the relative change in the populations of spherical and non-spherical voids as a function of temperature, we have calculated their asphericity as $\Delta R = R_f - R_v$, where:

$$R_f = \frac{3V_v}{S_v}, \text{ and} \quad (1)$$

$$R_v = \left(\frac{3V_v}{4\pi} \right)^{\frac{1}{3}}, \quad (2)$$

In the equations above, R_f and R_v are defined in terms of volume (V_v) and surface (S_v) of the voids such that large values of ΔR correspond to strongly non-spherical voids, while a perfectly spherical object would be characterized by $\Delta R=0$. As can be seen in Fig. 1b, the

probability density distribution of ΔR for voids in both room temperature and supercooled liquid water is clearly bi-modal. Furthermore, as we lower the temperature we observe a fattening of the tails for large values of ΔR , which suggest that voids in liquid water tend to become increasingly less spherical as we venture into the supercooled regimes.

The Percolating Voids Network

At this point, the statistics of these voids may not appear especially illuminating: after all, the changes as a function of supercooling seem to be rather small. The bare volumes of the voids however, does not shed light on possible correlations that exist between the voids. Furthermore, as we will see shortly, since the construction of the voids relies on the bottleneck radius (R_B), two voids in close proximity may not be merged if the gap between them is less than 1.1 \AA (see panel a of Fig. 2). This aspect cannot be captured by the statistics depicted in Fig. 1, and prompted us instead to look at connections between different voids.

If two voids are connected by means of an actual bottleneck (see panel a of Fig. 2), implying that they share a contact area large enough for a water molecule to move from one void to the other, the two voids are merged together into a single void. However, in some cases voids simply share one or more than one vertexes of their constituting polyhedra - without the existence of a real bottleneck between them (see panel a of Fig. 2). To investigate the implications of this possibility, we map the voids network onto a graph: we consider each void as a node of an undirected graph, and each connection (each shared vertex, or more than one, between two voids) as an edge of the same graph. Further details about this procedure can be found in Sec. .

This strategy allows us to pinpoint connected clusters of voids such as the one depicted in Fig. 2b: where disconnected and connected voids are depicted in orange and red, respectively. **This large connected void contains 385 spherical and non-spherical voids, which are shown with different intensity of red color (see Fig. 2b).** Another graphical way to represent these clusters of voids is shown in Fig. 2c: the graph illustrates the connectivity of the voids within

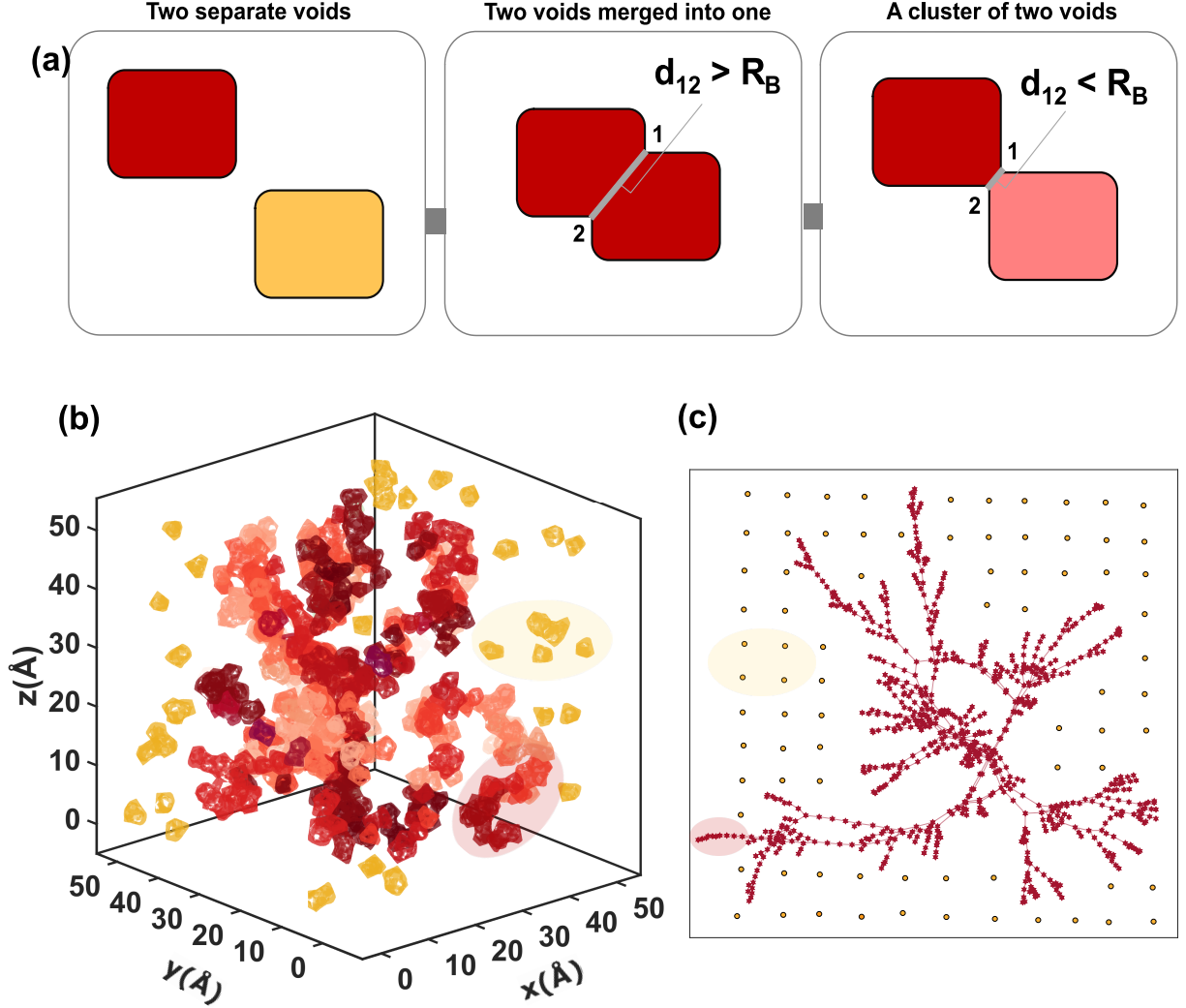


Figure 2: a) The schematic cartoon of two separate voids, two merged voids into one and a cluster of two connected voids, b) an example of connected and unconnected voids (cluster) in the supercooled liquid at $T=230$ K. The red color voids with different intensity contain 385 connected spherical and non-spherical voids along the simulation box (for clarity, we only show some). The orange color voids are example of unconnected voids, c) the graph plot of the connected and non-connected voids of panel a). A red graph here is made up of nodes (index of voids) which are connected by edges (red lines) and the orange graph has nodes with no edges.

a particular configuration of our models of supercooled liquid water: the red, connected nodes involve a combination of approximately 385 (both spherical and non-spherical voids) which form a large connected cluster spanning a sizable length scale (~ 8 nm). Isolated voids (unconnected clusters) are instead depicted as orange nodes on the grid in Fig. 2c. The yellow and red highlighted parts in panels b and c show a correspondence between voids and

nodes of a tree graph.

This analysis thus yields a mapping of the voids onto a network that allows us to identify clusters of connected voids. Various different properties of the clusters can now be examined including the total volume, number of voids and the asphericity of the cluster. The results are summarized in Fig. 3 for water at 300 K, 260 K and 230 K in panels a) through c). In each panel, we report the ΔR of the cluster as a function of the cluster size (given by the number of voids that constitute a given cluster). In addition, the top part of each panel illustrates a color map indicating the total volume of each cluster. For clarity, we note that the ΔR of the cluster involves determining the total volume and surface area given by the sum of contributions coming from individual voids in a cluster.

Each panel in Fig. 3 shows the presence of small and larger connected clusters - naturally the large clusters are characterized by larger volume and also by an enhanced asphericity. Interestingly, we see that as we go from 300 to 260 K and then finally to 230 K in supercooled water, there is a significant increase in the proportion of large connected clusters by an order of magnitude. As we will discuss in the next section, one of the issues we would like to explore, is to study whether water environments around isolated-disconnected voids are any different from those near large clusters of connected voids.

Motivated by the observations in Fig. 3, we focused on partitioning the void-space in *three small (SC)*, *intermediate (IC)* and *large (LC)* clusters. More specifically, we consider a cluster of voids to be large if all the clusters of voids having that particular cluster size are characterized by a value of ΔR greater than the maximum value of ΔR we have obtained for the unconnected clusters (i.e. cluster size=1). For instance, in Fig. 3c, the largest ΔR for the unconnected clusters is 2.83 Å: as such, only clusters of voids containing more than 17 voids are considered as large clusters. On the other hand, in the case of Fig. 3b, the largest ΔR for the unconnected clusters is 2.83 Å: as such, only clusters of voids containing more than 17 voids are considered as large clusters.

In order to appreciate the extent to which the voids percolate in the hydrogen bond

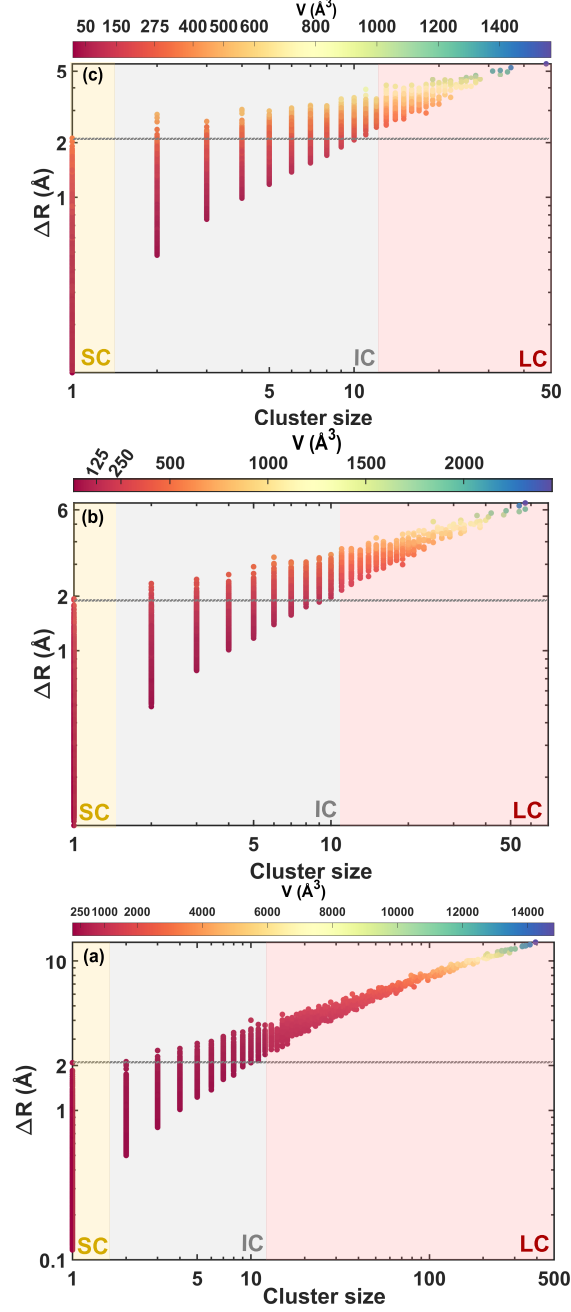


Figure 3: a) log-log plot of ΔR as a function of cluster size at a) $T=230$ K, b) $T=260$ K and c) $T=300$ K. The volume of clusters is shown in color code. The red transparent part shows the unconnected clusters with cluster size=1, and the red transparent part shows the large connected clusters.

network, we show in Fig. 4 the distribution associated with the longest length spanning the void⁴⁴ at 230 K, 260 K and 300 K. Fig. S1 in the SI shows that for the size of the small sized clusters span a length-scale similar to the length of a hydrogen bond and that this

doesn't change much upon supercooling. On the other hand, for the large clusters (Fig. 4), we observe there is a strong effect going from 260 to 230 K - the nucleation of voids results in clusters that can stretch over 8 nm in length. Given the finite size of our box and also the challenge in sampling these rare and long-length scale fluctuations, these effects are likely being underestimated.

The preceding analysis relies on partitioning the void network into small and larger clusters using a criterion that may seem rather arbitrary. However, using this criterion to distinguish between small and large clusters is rather physical since it results in a situation where there is no overlap in terms of ΔR between small and large clusters - as demonstrated in Fig. S2. In other words, small clusters of voids tend to be quite spherical overall, while large clusters of voids are highly non-spherical. We have also verified that modifying the criterion by which we identify a certain cluster of voids as small or large does not qualitatively change the main findings of our results.

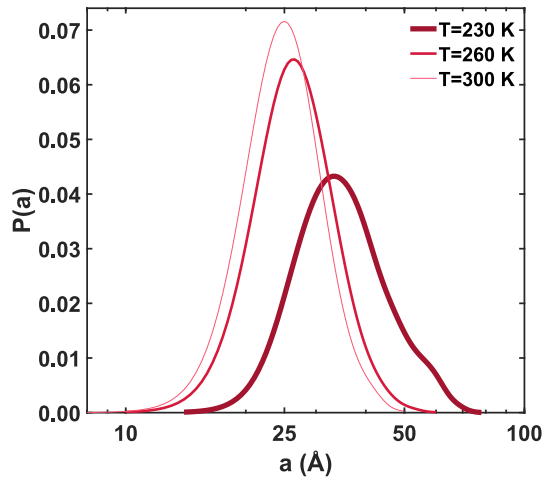


Figure 4: The longest distance between any two points forming the surface of large clusters at 230 K, 260 K and 300 K. The x-axis is in log scale.

The Water Network Near Voids

In the previous section, we established important signatures in the evolution of the void network upon supercooling. Using the distinction between small and large clusters of voids,

we assign each water molecule in our simulation box to a certain cluster of voids. This was achieved by determining the closest cluster that water molecules belong to. Using this criterion, we find that at 230 K about 20 and 46% of water molecules belong to small and large clusters respectively. As the temperature rises towards ambient conditions, this ratio changes to 52 and 2 % (see Table 1).

Table 1: Percentage of waters belong to small (SC), large (LC) and intermediate (IC) clusters at different temperatures.

LC %	SC %	IC %	T (K)
46	20	34	230
26	27	47	240
16	34	50	250
8	40	52	260
2	52	46	300

Up to this point in our discussion, we have not made any reference to fluctuations involving low and high density liquid. As pointed out earlier in the introduction, two of the most popular order parameters that are used to study the local structure of water and infer the presence of LDL and HDL water, are the local structure index (LSI) and the tetrahedrality (q) defined as:

$$\text{LSI} = \frac{1}{n} \sum_{i=1}^n (\Delta(i) - \bar{\Delta})^2 \quad \text{and} \quad (3)$$

$$q = 1 - \frac{3}{8} \sum_{j=1}^3 \sum_{k=j+1}^4 \left(\cos \Psi_{jk} + \frac{1}{3} \right)^2 \quad (4)$$

where $\Delta(i)$, $\bar{\Delta}$ and Ψ_{jk} correspond to the oxygen - oxygen distance between the i -th water molecule and its neighbors, the arithmetic mean of $\Delta(i)$ and the angle formed by the lines joining the oxygen atom of the water molecule under consideration and its nearest neighbor oxygen atoms j and k - respectively. Large values of q correspond to *more tetrahedral* water molecules while small values of the LSI correspond to water environments that are more

disordered and less ice-like. Next, we examined whether there was any correlation between these local order parameters and their proximity to the voids.

The **top** and **bottom** panels of Fig. 5 show the distributions of the LSI and tetrahedrality respectively, for water molecules belonging to small and large clusters at 230 K and 260 K. Firstly, as expected, there is an enhancement in the tetrahedrality of water upon supercooling. This is also reflected in the LSI distributions. Comparing the LSI and tetrahedrality of water molecules near small clusters (labeled SC) and large clusters (labeled LC), we observe that waters near the large voids are slightly more tetrahedral than those near small ones. This feature is also reflected in the LSI at 230 K and 260 K where we observe an enhancement in the tail of the distribution to lower values for water near the large clusters.

The LSI and q parameter do not interrogate fluctuations involving the topology of the hydrogen bond network. There have been several studies studying the how the distribution of closed rings in water evolve upon supercooling and in particular, how this is reflected in the presence of low and high density liquid. Car and co-workers³⁹ using ab initio molecular dynamics simulations, showed that rings associated with low density like water molecules (LSI values $< 0.13 \text{ \AA}^2$) are dominated by six membered rings, while in the case of high density like water (with LSI $> 0.13 \text{ \AA}^2$), the distribution of rings are much broader involving a fat tail to ring sizes bigger than 12. Using a similar criteria, Martelli⁴³ recently showed that under supercooling, the number of hexagonal rings increases.

In order to assess if the topology of the hydrogen bond network is different around small and large clusters, we determined the distribution of closed hydrogen bonded rings involving water molecules that lie within 2 \AA of the surface of the void. The left and right panels of Fig. 6 show the ring distributions around small and large voids. Interestingly, going from small to large clusters, we observe a shift in the balance between 6 and 7-membered rings. See the dotted bars of Fig. 6a and b. Larger percolating voids are surrounded by more hexagonal rings consistent with Refs. 39,43.

Besides the ring distributions, there are also other measures of changes in the topology

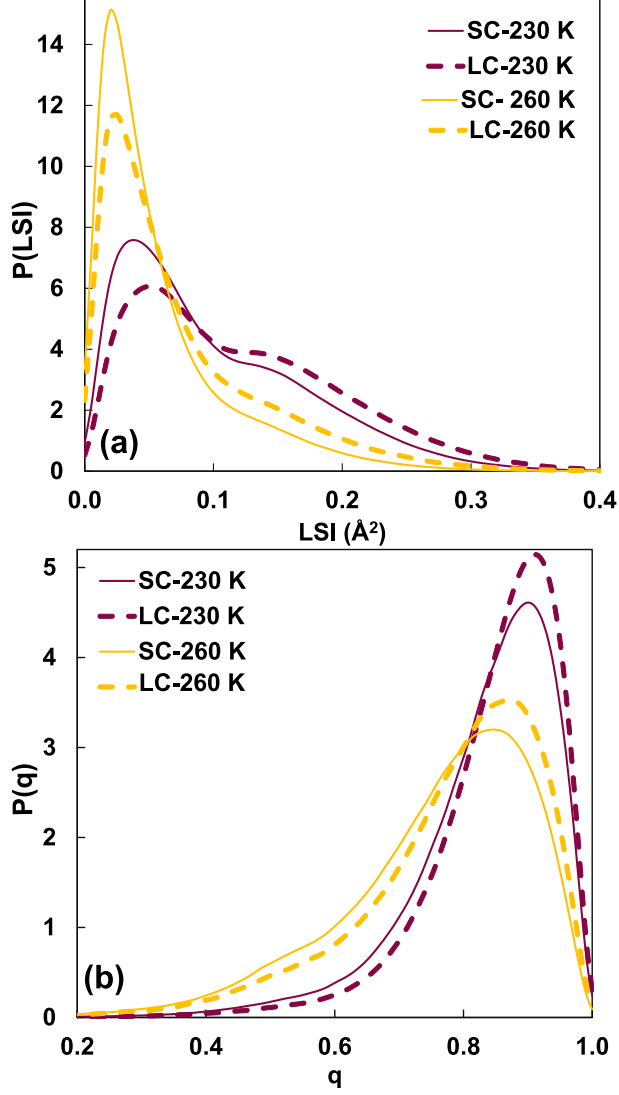


Figure 5: Distribution of (a) LSI and (b) q for waters in vicinity of small (SC) and large (LC) clusters at $T=230$ K (solid line) and $T=260$ K (dash line).

of the hydrogen bond network. In particular, local coordination defects have been shown to change under different thermodynamic conditions.⁷² We were curious to understand whether there would be any signature of the changes in the topology of the hydrogen bond network near the void network given by both small and big clusters. Interestingly, we find a larger population of both under- and over-coordinated water molecules in close vicinity to small clusters under supercooling - see panel c of Fig. 6 (see the right panel showing a cartoon representation of the various topological defects). In a very recent study, Markland and co-workers⁷³ have shown that as the temperature increases from supercooled water to beyond

ambient temperature, the population of coordinated (2A-2D) and under-coordinated (1A-2D, 2A-1D) water molecules decreases and increases respectively, while the over-coordinated (3A-2D) waters exhibits a maximum. They argue that these species can be correlated with the evolution of the Raman spectra upon supercooling. Our results are also consistent with their results and provide a more nuanced description of the fluctuations in the hydrogen bond network involving both the topological defects and the voids (see Fig. S3 in the SI).

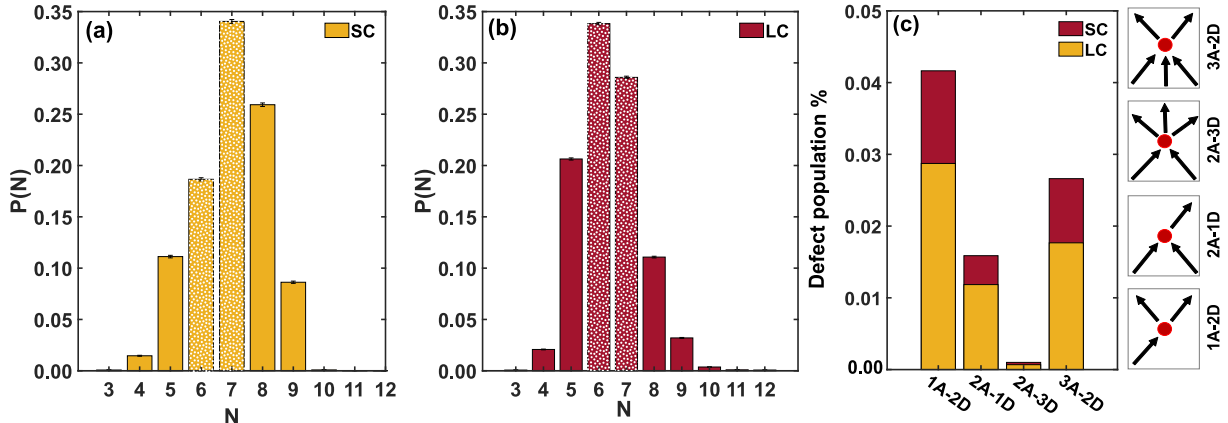


Figure 6: Probability distribution of N -membered primitive rings within 2 \AA from the surface of the a) small and b) large clusters at 230 K. The dotted bars show the 6- and 7-membered rings around small and large clusters, c) population of under- and over-coordinated topological defects associated with water molecules near small and large clusters at 230 K.

HD/LD Liquid Water and the Void Network

Earlier in the manuscript, we pointed out that many of the anomalies of water are thought to arise from the hypothesized second critical point, namely the LLCPP. The presence of an LLCPP is also consistent with the breakdown of the **Stokes-Einstein relationship** (SER) in the supercooled region of water.⁷⁴ The molecular origins of the LLCPP and its relationship with SER continues to be an open question.⁷⁴⁻⁸¹ In the following, we propose a possible link between the LLCPP, SER and the evolution of the void network in the supercooled regime.

Using a combination of both theory and experiments, Stanley and co-workers⁸² proposed a model based on the changes in the IR frequencies associated with essentially two populations of water molecules corresponding to LDA and HDA-like water as a function of

supercooling. Specifically, they found that at ~ 240 K, there was a cross over in the relative population of these two types of water molecules. These results are reproduced in the top left panel of Fig. 7. Using molecular dynamics simulations of TIP5P, they examined the evolution of the change in the tetrahedrality (q) parameter of the water molecules. By using a judicious choice of HD and LD waters based on their q value ($q > 0.8$ for LD and $q \leq 0.8$ for HD), they found that the relative concentration of these two species had a striking similarity to that obtained from the model built from the IR experiments.

Having observed some interesting trends between the LSI and q parameters of water molecules and their proximity to either small or large void clusters in Fig. 5, we were prompted to look into how the relative concentration of SC and LC water molecules changes upon supercooling. Although this analysis is essentially summarized in Table 1, to make a more direct comparison with Fig. 7a, we focused on the number of water molecules belong only to small (n_S) and large (n_L) clusters. The relative populations of the two classes of molecules can then be defined as $\frac{n_S}{N}$ and $\frac{n_L}{N}$, where $N = n_S + n_L$.

The relative populations of these two species are shown in the panel b of Fig. 7. The relative population of water molecules belonging to the intermediate cluster (IC) is reported in the color gray. For IC waters, the normalization of the population is with respect to all the water molecules. Interestingly, the qualitative behavior associated with the relative proportion of water molecules *belonging* to either SC and LC as a function of supercooling, is very similar to that observed by Stanley and co-workers (Fig. 7a). However, the structural factors that control the relative concentration of SC and LC waters is quite distinct. Our analysis suggests instead, that another possible order parameter involving the percolation of the voids and the water environments that surround them upon supercooling, has very similar behavior to the changes in the HD/LD waters. The percolation of the voids gives fresh insights into the collective nature of the density fluctuations upon supercooling. Local structural and topological changes in the hydrogen bond network also occur albeit in a much more subtle way as seen in Figs. 5 and 6.

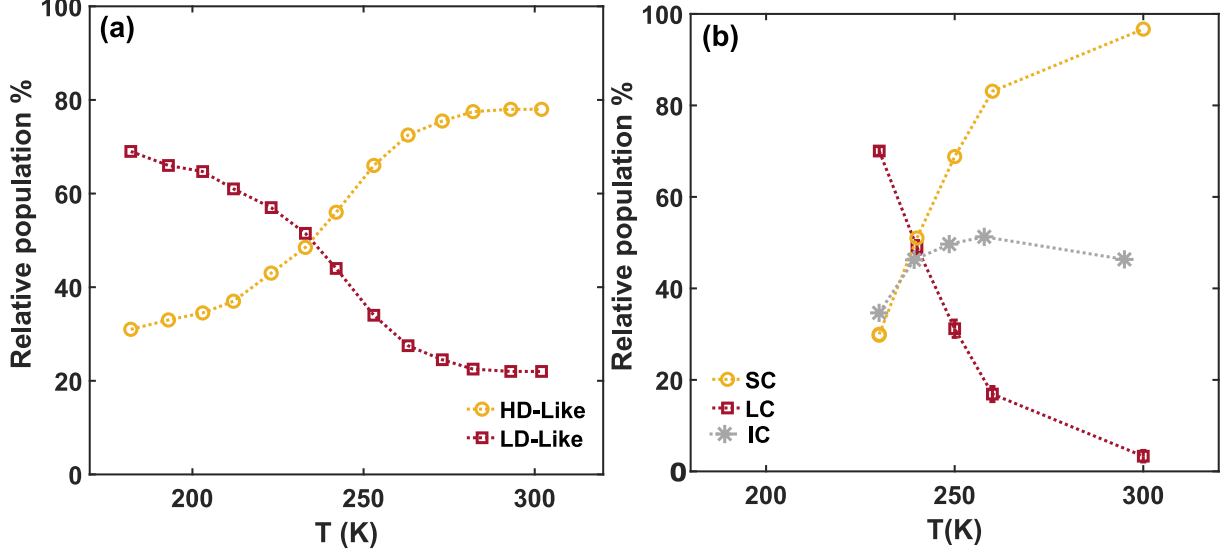


Figure 7: a) Relative population of HD and LD water with respect to the temperature from experiments of Ref. 82 and b) relative population of water molecules belong to small (SC) and large (LC) clusters. The relative population of water molecules belonging to intermediate cluster (IC) is reported in the color gray. The reader is reminded that these values for IC are normalized by the total number of waters.

The quantitative details involving the ratio of SC and LC water as a function of supercooling will of course, be sensitive to some of the the specific criterion used to distinguish between small and large clusters of voids as well as the choice of parameters such as R_B and R_P (see Sec.). However, we have checked that the qualitative trends we have found are robust with respect to these technicalities (see Figs. S4-S5 in SI).

Conclusions

The molecular origins of density fluctuations in water and how they change across its phase diagram, has been a topic of intense study and debate in the field. A lot of our knowledge on the microscopic interpretations of waters anomalies relies on the existence of two limiting states of water: high and low density which differ in the local coordination environment.

In some of our recent work,^{44,47} we have shown that there is a lot important information lying in the correlations between the hydrogen bond network of water and the nature of

empty space that is carved out within it. Specifically, Voronoi voids provide a rather powerful theoretical tool to quantify the empty space in liquid water and also identify high and low density regions in water that occur on a much longer length scale than those predicted by local order parameters such as LSI and q .

Here, demonstrate that investigating the structural properties of the regions of empty space within the liquid network leads to a nuanced and rich description of the behavior of supercooled water. In particular, we show that upon supercooling, there is a subtle increase in the fraction of free volume in the liquid which is manifested in the creation of larger delocalized voids, as well as the nucleation of smaller voids to form large connected clusters of empty space.

Intriguingly, by assigning all water molecules to either small isolated spherical voids or large non-spherical clusters of many voids, we are able to identify water molecules that are more or less tetrahedral, respectively. In the former case, the size of closed rings is dominated by hexagon, with fewer under- and over-coordinated topological defected waters, while in the latter case the 7-members rings are more dominated with a higher percentage of topological defects. The study of percolating Voronoi networks and its role in creating low and high density regions has previously been noted by Medvedev and co-workers⁸³ using molecular dynamics simulations of liquid and quenched rubidium.

Interestingly, by examining the evolution of the ratio of LD is also consistent with previous findings reported in Ref. 82 which suggests that collective behavior associated with the fluctuations in the empty space may have important bearing on the SER breakdown. This is reinforced further, by other studies showing that fractional SER in metallic glasses is coupled with the formation of large clusters of trapped atoms that percolate through the liquid.^{84,85}

Our results thus shed new light onto the structural properties of supercooled water, by means of a framework that steps away from the current paradigm of local order parameters to embrace the full complexity of the water network including the evolution of the empty space as well as topological properties of the HB network.

References

- (1) Bengtzelius, U.; Gotze, W.; Sjolander, A. Dynamics of supercooled liquids and the glass transition. *J. Phys. C: Sol. stat. Phys.* **1984**, *17*, 5915.
- (2) Ediger, M. D. Spatially heterogeneous dynamics in supercooled liquids. *Ann. Rev. Phys. Chem.* **2000**, *51*, 99–128.
- (3) Bakhach, J. The cryopreservation of composite tissues: principles and recent advancement on cryopreservation of different type of tissues. *Organogenesis* **2009**, *5*, 119–126.
- (4) Bartels-Rausch, T. Chemistry: Ten things we need to know about ice and snow. *Nature* **2013**, *494*, 27.
- (5) Gallo, P.; Amann-Winkel, K.; Angell, C. A.; Anisimov, M. A.; Caupin, F.; Chakravarty, C.; Lascaris, E.; Loerting, T.; Panagiotopoulos, A. Z.; Russo, J., et al. Water: A tale of two liquids. *Chem. Rev.* **2016**, *116*, 7463–7500.
- (6) Soper, A. K.; Ricci, M. A. Structures of high-density and low-density water. *Phys. Rev. Lett.* **2000**, *84*, 2881.
- (7) Koga, K.; Tanaka, H.; Zeng, X. C. First-order transition in confined water between high-density liquid and low-density amorphous phases. *Nature* **2000**, *408*, 564.
- (8) Finney, J.; Hallbrucker, A.; Kohl, I.; Soper, A.; Bowron, D. Structures of high and low density amorphous ice by neutron diffraction. *Phys. Rev. Lett.* **2002**, *88*, 225503.
- (9) Mallamace, F.; Broccio, M.; Corsaro, C.; Faraone, A.; Majolino, D.; Venuti, V.; Liu, L.; Mou, C.-Y.; Chen, S.-H. Evidence of the existence of the low-density liquid phase in supercooled, confined water. *Proc. Natl. Acad. Sci.* **2007**, *104*, 424–428.
- (10) Saitta, A. M.; Datchi, F. Structure and phase diagram of high-density water: The role of interstitial molecules. *Phys. Rev. E* **2003**, *67*, 020201.

- (11) Poole, P. H.; Sciortino, F.; Essmann, U.; Stanley, H. E. Phase behaviour of metastable water. *Nature* **1992**, *360*, 324.
- (12) English, N. J.; Tse, J. S. Density Fluctuations in Liquid Water. *Phys. Rev. Lett.* **2011**, *106*, 037801.
- (13) Brovchenko, I.; Geiger, A.; Oleinikova, A. Liquid-liquid phase transitions in supercooled water studied by computer simulations of various water models. *J. Chem. Phys.* **2005**, *123*, 044515.
- (14) English, N. J.; John, S. T. Density fluctuations in liquid water. *Phys. Rev. Lett.* **2011**, *106*, 037801.
- (15) Mishima, O.; Suzuki, Y. Propagation of the polyamorphic transition of ice and the liquid-liquid critical point. *Nature* **2002**, *419*, 599.
- (16) Mishima, O. Liquid-liquid critical point in heavy water. *Phys. Rev. Lett.* **2000**, *85*, 334.
- (17) Kanno, H.; Miyata, K. The location of the second critical point of water. *Chem. Phys. Lett.* **2006**, *422*, 507–512.
- (18) Mallamace, F.; Corsaro, C.; Broccio, M.; Branca, C.; Gonzalez-Segredo, N.; Spooren, J.; Chen, S.-H.; Stanley, H. NMR evidence of a sharp change in a measure of local order in deeply supercooled confined water. *Proc. Natl. Acad. Sci. U. S. A.* **2008**, *105*, 12725–12729.
- (19) Sellberg, J. A.; Huang, C.; McQueen, T. A.; Loh, N.; Laksmono, H.; Schlesinger, D.; Sierra, R.; Nordlund, D.; Hampton, C.; Starodub, D., et al. Ultrafast X-ray probing of water structure below the homogeneous ice nucleation temperature. *Nature* **2014**, *510*, 381.
- (20) Sellberg, J. A.; Kaya, S.; Segtnan, V. H.; Chen, C.; Tyliczszak, T.; Ogasawara, H.; Nordlund, D.; Pettersson, L. G.; Nilsson, A. Comparison of x-ray absorption spectra

- between water and ice: New ice data with low pre-edge absorption cross-section. *J. Chem. Phys.* **2014**, *141*, 034507.
- (21) Palmer, J. C.; Martelli, F.; Liu, Y.; Car, R.; Panagiotopoulos, A. Z.; Debenedetti, P. G. Metastable liquid–liquid transition in a molecular model of water. *Nature* **2014**, *510*, 385.
- (22) Xu, L.; Kumar, P.; Buldyrev, S. V.; Chen, S.-H.; Poole, P. H.; Sciortino, F.; Stanley, H. E. Relation between the Widom line and the dynamic crossover in systems with a liquid–liquid phase transition. *Proc. Natl. Acad. Sci. U. S. A.* **2005**, *102*, 16558–16562.
- (23) Abascal, J. L.; Vega, C. Widom line and the liquid–liquid critical point for the TIP4P/2005 water model. *J. Chem. Phys.* **2010**, *133*, 234502.
- (24) Liu, Y.; Palmer, J. C.; Panagiotopoulos, A. Z.; Debenedetti, P. G. Liquid-liquid transition in ST2 water. *J. Chem. Phys.* **2012**, *137*, 214505.
- (25) Corradini, D.; Rovere, M.; Gallo, P. Structural properties of high and low density water in a supercooled aqueous solution of salt. *J. Phys. Chem. B* **2011**, *115*, 1461–1468.
- (26) Li, Y.; Li, J.; Wang, F. Liquid–liquid transition in supercooled water suggested by microsecond simulations. *Proc. Natl. Acad. Sci. U. S. A.* **2013**, *110*, 12209–12212.
- (27) Palmer, J. C.; Car, R.; Debenedetti, P. G. The liquid–liquid transition in supercooled ST2 water: a comparison between umbrella sampling and well-tempered metadynamics. *Faraday discuss.* **2013**, *167*, 77–94.
- (28) Smallenburg, F.; Filion, L.; Sciortino, F. Erasing no-man’s land by thermodynamically stabilizing the liquid–liquid transition in tetrahedral particles. *Nature Phys.* **2014**, *10*, 653.
- (29) Ni, Y.; Skinner, J. Evidence for a liquid-liquid critical point in supercooled water within the E3B3 model and a possible interpretation of the kink in the homogeneous nucle-

ation line. *J. Chem. Phys.*, volume=144, number=21, pages=214501, year=2016, publisher=AIP Publishing

- (30) Biddle, J. W.; Singh, R. S.; Sparano, E. M.; Ricci, F.; González, M. A.; Valeriani, C.; Abascal, J. L.; Debenedetti, P. G.; Anisimov, M. A.; Caupin, F. Two-structure thermodynamics for the TIP4P/2005 model of water covering supercooled and deeply stretched regions. *J. Chem. Phys.* **2017**, *146*, 034502.
- (31) Mishima, O.; Calvert, L.; Whalley, E. An apparently first-order transition between two amorphous phases of ice induced by pressure. *Nature* **1985**, *314*, 76.
- (32) Mishima, O. Reversible first-order transition between two H₂O amorphs at 0.2 GPa and 135 K. *J. Chem. Phys.* **1994**, *100*, 5910–5912.
- (33) Klotz, S.; Strässle, T.; Nelmes, R.; Loveday, J.; Hamel, G.; Rousse, G.; Canny, B.; Chervin, J.; Saitta, A. Nature of the polyamorphic transition in ice under pressure. *Phys. Rev. Lett.* **2005**, *94*, 025506.
- (34) Walrafen, G. Raman spectral studies of water structure. *J. Chem. Phys.* **1964**, *40*, 3249–3256.
- (35) Walrafen, G. Raman spectral studies of the effects of temperature on water structure. *J. Chem. Phys.* **1967**, *47*, 114–126.
- (36) Walrafen, G.; Fisher, M.; Hokmabadi, M.; Yang, W.-H. Temperature dependence of the low-and high-frequency Raman scattering from liquid water. *J. Chem. Phys.* **1986**, *85*, 6970–6982.
- (37) Woutersen, a.; Emmerichs, U.; Bakker, H. Femtosecond mid-IR pump-probe spectroscopy of liquid water: Evidence for a two-component structure. *Science* **1997**, *278*, 658–660.

- (38) The inhomogeneous structure of water at ambient conditions. *Proc. Natl. Acad. Sci. U. S. A.* **2009**, *106*, 15214–15218.
- (39) Santra, B.; DiStasio Jr, R. A.; Martelli, F.; Car, R. Local structure analysis in ab initio liquid water. *Molecular Phys.* **2015**, *113*, 2829–2841.
- (40) Shiratani, E.; Sasai, M. Growth and collapse of structural patterns in the hydrogen bond network in liquid water. *J. Chem. Phys.* **1996**, *104*, 7671–7680.
- (41) Chau, P.-L.; Hardwick, A. A new order parameter for tetrahedral configurations. *Mol. Phys.* **1998**, *93*, 511–518.
- (42) Errington, J. R.; Debenedetti, P. G. Relationship between structural order and the anomalies of liquid water. *Nature* **2001**, *409*, 318–321.
- (43) Martelli, F. Unravelling the contribution of local structures to the anomalies of water: The synergistic action of several factors. *J. Chem. Phys.* **2019**, *150*, 094506.
- (44) Ansari, N.; Dandekar, R.; Caravati, S.; Sosso, G.; Hassanali, A. High and low density patches in simulated liquid water. *J. Chem. Phys.* **2018**, *149*, 204507.
- (45) Sastry, S.; Corti, D. S.; Debenedetti, P. G.; Stillinger, F. H. Statistical geometry of particle packings. I. Algorithm for exact determination of connectivity, volume, and surface areas of void space in monodisperse and polydisperse sphere packings. *Phys. Rev. E* **1997**, *56*, 5524.
- (46) Hassanali, A. A.; Giberti, F.; Sosso, G. C.; Parrinello, M. The role of the umbrella inversion mode in proton diffusion. *Chem. Phys. Lett.* **2014**, *599*, 133 – 138.
- (47) Sosso, G. C.; Caravati, S.; Rotskoff, G.; Vaikuntanathan, S.; Hassanali, A. On the role of nonspherical cavities in short length-scale density fluctuations in water. *J. Phys. Chem. A* **2016**, *121*, 370–380.

- (48) Ansari, N.; Laio, A.; Hassanali, A. A. Spontaneously Forming Dendritic Voids in Liquid Water Can Host Small Polymers. *J. Phys. Chem. Lett.* **2019**, *10*, 5585.
- (49) Abascal, J.; Sanz, E.; García Fernández, R.; Vega, C. A potential model for the study of ices and amorphous water: TIP4P/Ice. *J Chem. Phys.* **2005**, *122*, 234511.
- (50) Fitzner, M.; Sosso, G. C.; Cox, S. J.; Michaelides, A. Ice is born in low-mobility regions of supercooled liquid water. *Proc. Natl. Acad. Sci.* **2019**, *116*, 2009–2014.
- (51) Abraham, M. J.; Murtola, T.; Schulz, R.; Páll, S.; Smith, J. C.; Hess, B.; Lindahl, E. GROMACS: High performance molecular simulations through multi-level parallelism from laptops to supercomputers. *SoftwareX* **2015**, *1*, 19–25.
- (52) Pedevilla, P.; Fitzner, M.; Sosso, G. C.; Michaelides, A. Heterogeneous seeded molecular dynamics as a tool to probe the ice nucleating ability of crystalline surfaces. *J. Chem. Phys.* **2018**, *149*, 072327.
- (53) Espinosa, J. R.; Vega, C.; Sanz, E. Ice-Water Interfacial Free Energy for the TIP4P, TIP4P/2005, TIP4P/Ice, and mW Models As Obtained from the Mold Integration Technique. *J. Phys. Chem. C* **2016**, *120*, 8068–8075.
- (54) Babin, V.; Medders, G. R.; Paesani, F. Toward a universal water model: First principles simulations from the dimer to the liquid phase. *J. Phys. Chem. Lett.* **2012**, *3*, 3765.
- (55) Babin, V.; Leforestier, C.; Paesani, F. Development of a “First principles” water potential with flexible monomers. II: trimer potential energy surface, third virial coefficient, and Small clusters. *J. Chem. Theory Comput.* **2014**, *9*, 5395.
- (56) Medders, G. R.; Babin, V.; Paesani, F. Development of a “first-principles” water potential with flexible monomers. III. Liquid phase properties. *J. Chem. Theory Comput.* **2014**, *10*, 2906.

- (57) Miyamoto, S.; Kollman, P. A. SETTLE: an analytical version of the SHAKE and RATTLE algorithm for rigid water models. *J. Comput. Chem.* **1992**, *13*, 952–962.
- (58) Hess, B.; Bekker, H.; Berendsen, H. J. C.; Fraaije, J. G. E. M. LINCS: a linear constraint solver for molecular simulations. *J. Comput. Chem.* **1997**, *18*, 1463–1472.
- (59) Hess, B. P-LINCS: A Parallel Linear Constraint Solver for Molecular Simulation. *J. Chem. Theory Comput.* **2008**, *4*, 116–122.
- (60) Essmann, U.; Perera, L.; Berkowitz, M. L.; Darden, T.; Lee, H.; Pedersen, L. G. A smooth particle mesh Ewald method. *J. Chem. Phys.* **1995**, *103*, 8577–8593.
- (61) Swope, W.; Andersen, H.; Berens, P.; Wilson, K. A computer-simulation method for the calculation of equilibrium-constants for the formation of physical clusters of molecules: Application to small water clusters. *J. Chem. Phys.* **1982**, *76*, 637–649.
- (62) Nosé, S.; Klein, M. Constant pressure molecular dynamics for molecular systems. *Mol. Phys.* **1983**, *50*, 1055–1076.
- (63) Hoover, W. G. Canonical dynamics: equilibrium phase-space distributions. *Phys. Rev. A* **1985**, *31*, 1695.
- (64) Berendsen, H. J.; Postma, J. v.; van Gunsteren, W. F.; DiNola, A.; Haak, J. Molecular dynamics with coupling to an external bath. *J. Chem. Phys.* **1984**, *81*, 3684–3690.
- (65) Parrinello, M.; Rahman, A. Polymorphic transitions in single crystals: A new molecular dynamics method. *J. Appl. Phys.* **1981**, *52*, 718–7190.
- (66) Alinchenko, M. G.; Anikeenko, A. V.; Medvedev, N. N.; Voloshin, V. P.; Mezei, M.; Jedlovsky, P. Morphology of voids in molecular systems. A voronoi- delaunay analysis of a simulated DMPC membrane. *J. Phys. Chem. B* **2004**, *108*, 19056–19067.
- (67) The VNP code, <http://www.kinetics.nsc.ru/mds/?Software:VNP>. <http://www.kinetics.nsc.ru/mds/?Software:VNP>, 2016; Accessed: 05-07-2016.

- (68) Le Roux, S.; Jund, P. Ring statistics analysis of topological networks: New approach and application to amorphous GeS₂ and SiO₂ systems. *Comput. Mater. Sci.* **2010**, *49*, 70–83.
- (69) Bakó, I.; Bencsura, Á.; Hermansson, K.; Bálint, S.; Grósz, T.; Chihaiia, V.; Oláh, J. Hydrogen bond network topology in liquid water and methanol: a graph theory approach. *Phys. Chem. Chem. Phys.* **2013**, *15*, 15163–15171.
- (70) Tarjan, R. Depth-first search and linear graph algorithms. *SIAM J. Comput.* **1972**, *1*, 146–160.
- (71) MATLAB and Statistics Toolbox Release 2017a, The MathWorks, Inc., Natick, Massachusetts, United States, 2017.
- (72) Gasparotto, P.; Hassanali, A. A.; Ceriotti, M. Probing defects and correlations in the hydrogen-bond network of ab initio water. *J. Chem. Theory Comput.* **2016**, *12*, 1953–1964.
- (73) Morawietz, T.; Urbina, A. S.; Wise, P. K.; Wu, X.; Lu, W.; Ben-Amotz, D.; Markland, T. E. Hiding in the crowd: Spectral signatures of overcoordinated hydrogen bond environments. *J. Phys. Chem. Lett.* **2019**, *10*, 6067.
- (74) Kumar, P.; Buldyrev, S.; Becker, S.; Poole, P.; Starr, F.; Stanley, H. Relation between the Widom line and the breakdown of the Stokes–Einstein relation in supercooled water. *Proc. Natl. Acad. Sci.* **2007**, *104*, 9575–9579.
- (75) Tarjus, G.; Kivelson, D. Breakdown of the Stokes–Einstein relation in supercooled liquids. *J. Chem. Phys.* **1995**, *103*, 3071–3073.
- (76) Chen, S.-H.; Mallamace, F.; Mou, C.-Y.; Broccio, M.; Corsaro, C.; Faraone, A.; Liu, L. The violation of the Stokes–Einstein relation in supercooled water. *Proc. Natl. Acad. Sci.* **2006**, *103*, 12974–12978.

- (77) Mallamace, F.; Branca, C.; Corsaro, C.; Leone, N.; Spooren, J.; Stanley, H. E.; Chen, S.-H. Dynamical crossover and breakdown of the Stokes- Einstein relation in confined water and in methanol-diluted bulk water. *J. Phys. Chem. B* **2010**, *114*, 1870–1878.
- (78) Jung, Y.; Garrahan, J. P.; Chandler, D. Excitation lines and the breakdown of Stokes-Einstein relations in supercooled liquids. *Phys. Rev. E* **2004**, *69*, 061205.
- (79) Cervený, S.; Mallamace, F.; Swenson, J.; Vogel, M.; Xu, L. Confined water as model of supercooled water. *Chem. Rev.* **2016**, *116*, 7608–7625.
- (80) Kumar, P. Breakdown of the Stokes–Einstein relation in supercooled water. *Proc. Natl. Acad. Sci.* **2006**, *103*, 12955–12956.
- (81) Stillinger, F. H. A topographic view of supercooled liquids and glass formation. *Science* **1995**, *267*, 1935–1939.
- (82) Xu, L.; Mallamace, F.; Yan, Z.; Starr, F. W.; Buldyrev, S. V.; Stanley, H. E. Appearance of a fractional Stokes–Einstein relation in water and a structural interpretation of its onset. *Nature Phys.* **2009**, *5*, 565.
- (83) Medvedev, N. N.; Geiger, A.; Brostow, W. Distinguishing liquids from amorphous solids: Percolation analysis on the Voronoi network. *J. Chem. Phys.* **1990**, *93*, 8337–8342.
- (84) Charbonneau, P.; Jin, Y.; Parisi, G.; Zamponi, F. Hopping and the Stokes–Einstein relation breakdown in simple glass formers. *Proc. Natl. Acad. Sci. U. S. A.* **2014**, *111*, 15025–15030.
- (85) Pan, S.; Wu, Z.; Wang, W.; Li, M.; Xu, L. Structural origin of fractional Stokes-Einstein relation in glass-forming liquids. *Sci. Rep.* **2017**, *7*, 39938.